The alkyl-connected 2-amino-6-vinylpurine (AVP) crosslinking agent for improved selectivity to the cytosine base in RNA

Yosuke Taniguchi [a,c], Yusuke Kurose [a], Takamasa Nishioka [a], Fumi Nagatsugi [b,c], Shigeki Sasaki [a,c,*]

[a] Graduate School of Pharmaceutical Sciences, Kyushu University, 3-1-1 Maidashi, Higashi-ku, Fukuoka 812-8582, Japan
[b] Institute of Multidisciplinary Research for Advanced Materials, Tohoku University, 2-1-1 Katahira, Aoba-ku, Sendai-shi, Miyagi 98-8587, Japan
[c] CREST, Japan Science and Technology Agency, Japan

ARTICLE INFO

ABSTRACT

We have previously reported that the 2-amino-6-vinylpurine (AVP) nucleoside exhibits a highly efficient and selective crosslinking reaction toward cytosine and displayed an improved antisense inhibition in cultured cells. In this study, we further investigated the alkyl-connected AVP nucleoside analogs for more efficient crosslinking to the cytosine base (rC) of the target RNA. We synthesized three AVP analogs which connect the 2-amino-6-vinylpurine unit to the 2′-deoxyribose through a methylene, an ethylene, or a butylene linker. The ODN incorporating the AVP analog with the methylene or the butylene linker showed a slightly higher crosslinking to the target rC of RNA than the original AVP with no linker. In contrast, the AVP with the ethylene linker formed a selective and efficient crosslink to the rC of the target RNA.

© 2010 Elsevier Ltd. All rights reserved.

1. Introduction

RNA interactive oligonucleotides have significant potentials as therapeutic agents for the treatment of a number of diseases, such as cancers, diabetes, and infectious diseases.[1–7] Their clinical applications have attracted more and more attention since the discovery of the intrinsic and significant roles of non-coding functional RNAs in the regulation of the gene expression in living cells. Among the RNA binding molecules, the antisense oligonucleotides (ASO) have the longest research history for therapeutic applications. A variety of chemical modifications have been made on the natural-type ASO for their in vivo use, such as the phosphorothioate backbone (PS-oligonucleotide), 2′-O-methyl (2′-OMe), 2′-O-methoxyethyl (2′-MOE), and 2′-O-4′-C methylene locked nucleic acid (LNA) modified nucleotides.[8–11] These modifications are beneficial for the tolerance to nucleases, thermal stability of the complex with target RNAs, or penetration into cells. Another interesting strategy of ASO is the use of chemically reactive nucleotide analogs for the stabilization of the complex with the target RNA by forming a covalent bond. Psolaren photo-crosslinking units have been widely used in biological studies. We have developed the original crosslinking agent, the 2-amino-6-vinylpurine nucleoside analog (AVP), for the selective crosslinking reaction with the cytosine base (Scheme 1). Its stable precursor, the 2-amino-6-phenylthioethylpurine nucleoside (AVP (SPh)), has exhibited an
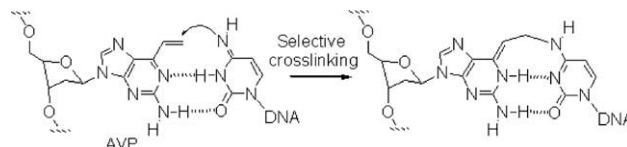

Scheme 1. Predicted alkylation reaction of AVP (2-amino-6-alkyl-purine) and cytosine in duplex DNA.

improved antisense inhibition through automatic activation within the complex with the target RNA.[12–15] This 'induced alkylating system' has been further applied to intracellular antisense inhibition, in which the ASO containing AVP (SMe) was conjugated with PEG and formulated into nano-particles of the polyion complex micelles with poly-L-lysine.[16] The AVP derivatives have other applications in the post-synthetic conjugation and in the DNA polymerase reaction.[17–19] However, it was realized in subsequent studies that the reactivity of AVP depends on the target RNA sequence. It was hypothesized that the local structure of the DNA/RNA heteroduplex slightly varies with the change in the sequence and affects the closeness between the vinyl group of AVP and the amino group of the cytosine base. Thus, the new AVP derivatives were designed to have a spacer between the 2-amino-6-vinylpurine unit and 2′-deoxyribose by expecting improvement in the proximity effect to the cytosine base (Fig. 1). The AVP analogs are called o-AVP with no linker (original), me-AVP with the methylene linker, et-AVP with the ethylene linker and bu-AVP with the butylene linker. In our earlier study, et-AVP and bu-AVP were used for the selective crosslinking to the adenine base of the TA pair, and the cytosine

---

* Corresponding author. Tel./fax: +81 92 642 6651.
  E-mail address: sasaki@phar.kyushu-u.ac.jp (S. Sasaki).
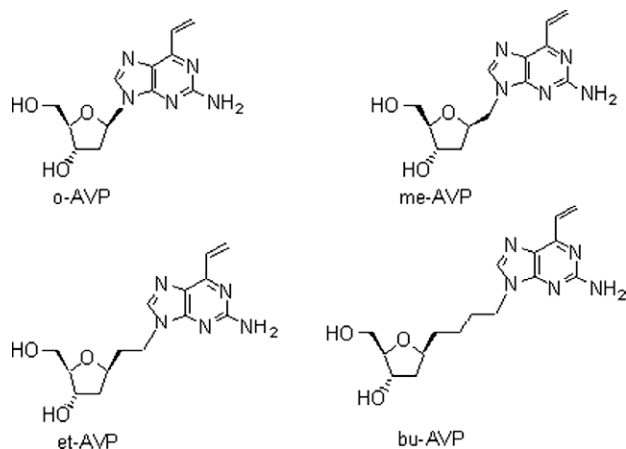
Figure 1. Structures of AVP analog monomers bearing alkyl linker between AVP and 20f-deoxyribose.

base of the GC pair in the triplex DNA, respectively.[20–22] In this paper, we describe in detail the synthesis of the linker-containing AVP analogs, and evaluation of the crosslinking properties of the oligonucleotides incorporating them.

2. Result

2.1. Synthesis

2.1.1. Synthesis of the methylene-linked 2-amino-6-vinylpurine derivative (me-AVP-SMe)

The synthesis of the new nucleoside analog, the methylene-linked 2-amino-6-vinylpurine derivative **4**, is shown in Scheme 2. 1′-β-Cyano-2′-deoxyribose **1**[23] was converted to the tosylated sugar unit **2** in 66% yield by a sequence of reactions including hydrolysis,[24] reduction of the resulting carboxylic acid using borate, and subsequent treatment with tosylchloride. The displacement of the tosylate group of **2** with 6-chloro-2-aminopurine afforded the 7 N-alkylated product as the major product in 68% after purification by silica-gel column chromatography (7 N/9 N > 49:1). The Pd(II)-catalyzed cross-coupling reaction with the 2,4,6-trivinylcyclotriboroxane pyridine complex[25] gave the 2-amino-6-vinylpurine (AVP) derivative, which afforded **3** by the reaction with NaSMe. After removal of the toluoyl protecting groups, the corresponding diol groups were transiently protected with TMS groups,[26] followed by protection of the 2-amino group with phenoxyacetyl chloride to produce **4** (me-AVP-SMe) in 68% yield from **3** in two steps. The synthesis of et-AVP-SMe and bu-AVP-SMe was performed as previously reported.[21,22] The abbreviation –SMe represents the fact that the vinyl group of AVP is protected by the methylsulfide group.

2.1.2. Synthesis of the amidite precursor and the oligonucleotide containing the AVP derivative

As shown in Scheme 3, the diol compounds **4** (o-, me-, et-, and bu-AVP-SMe) were converted to the corresponding phosphorami-

dite precursors **5** by the conventional method. The phosphoramidite precursors (**5**) were incorporated into ODNs using the DNA automated synthesizer. The synthesized ODNs **6** were purified by HPLC, the DMTr-protecting group was removed in an aqueous AcOH solution, and their structures were identified by MALDI-TOF MS measurements. These results are summarized in Table 1. The purified ODNs were treated with magnesium monoperoxyphthalate (MMPP) followed by treatment with an aqueous NaOH solution to generate the vinyl group of ODNs **7**, which were purified by HPLC again, and confirmed by a MALDI-TOF MS measurement (data not shown).

2.2. Estimation of crosslinking reactions with oligonucleotides containing AVP derivatives for DNA or RNA

The crosslinking reactions of 16 mer ODNs, o-ODN(**8**), me-ODN (**8**), et-ODN(**8**), and bu-ODN(**8**) containing AVP were performed using the FAM-labeled complementary DNA and RNA, and its progress was followed by the denatured gel mobility shift assay including 7 M urea. The yield of the crosslinked products were determined by quantification of the fluorescent bands based on the bands corresponding to the non-reacted target DNA and RNA Examples of the gel results of the o-ODN(**8**)/RNA and et-ODN(**8**)/RNA heteroduplex are shown in Figure 2. The time-dependent changes in the obtained alkylation yields are summarized in Figure 3. Previously, we reported that ODN having the original structure of AVP, o-ODN(**8**), exhibited a highly efficient and selective crosslinking reaction toward dC in the complimentary DNA (Fig. 3A). However, almost no crosslinking ability by o-ODN(**8**) was observed for any base in the target RNA (Figs. 2A and 3E). As the reactivity of the vinyl group of AVP is highly dependent on the distance to the amino group, these results indicate that the proximity effect between AVP and rC is lost in the DNA/RNA hetero duplex of this sequence. The ODN me-ODN(**8**) with AVP connected by the methyl linker showed less reactivity and specificity in the crosslinking reaction with the DNA targets, and displayed only a negligible reactivity to the RNA targets (Fig. 3B and F). In a remarkable contrast, et-ODN(**8**) including AVP connected by the ethyl linker exhibited a high crosslinking reactivity with a high selectivity to rC in DNA/RNA hetero duplex (Figs. 2B and 3G), although a lower reactivity and selectivity were observed to the DNA targets (Fig. 3C). The ODN bu-ODN(**8**) did not show any significant crosslinking reactivity either to the DNA or the RNA targets (Fig. 3D and H). These results clearly indicated that the optimal length of the spacer between the AVP unit and the 2′-deoxyribose group is the ethylene linker for the rC of DNA/RNA sequences used in this study.

As RNA generally forms a secondary structure under physiological conditions, we tested the crosslinking ability of the alkyl-linked AVP structure to the 27 mer RNA target with a hairpin-loop structure using o-ODN(**9**) and et-ODN(**9**), which have the AVP unit at the complementary site toward the rC in the loop position of the RNA target (Fig. 4A). As predicted from the results of Figure 3E, o-ODN(**9**) did not show a high reactivity to this loop RNA target (Fig. 4B). On the other hand, et-ODN(**9**)
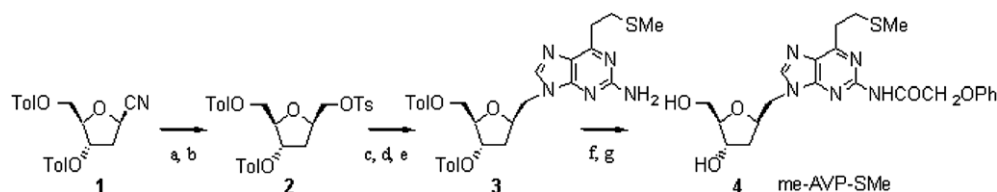
Scheme 2. Reagents and conditions: (a) (1) concd HCl–dioxane; (2) BH₃–THF, dry THF 80% (two steps); (b) p-TsCl, dry pyridine 82%; (c) 2-amino-6-chloropurine, t-BuOK, dry DMSO 68%; (d) Pd(PPh₃)₄, vinylboronic anhydride, LiBr, K₂CO₃, H₂O/dioxane; (e) MeSNa, CH₃CN 97% (two steps); (f) NaOMe, dry MeOH; (g) TMSCl, dry pyridine, dry CH₂Cl₂; (2) PhOAcCl; (3) MeOH 68% (two steps).
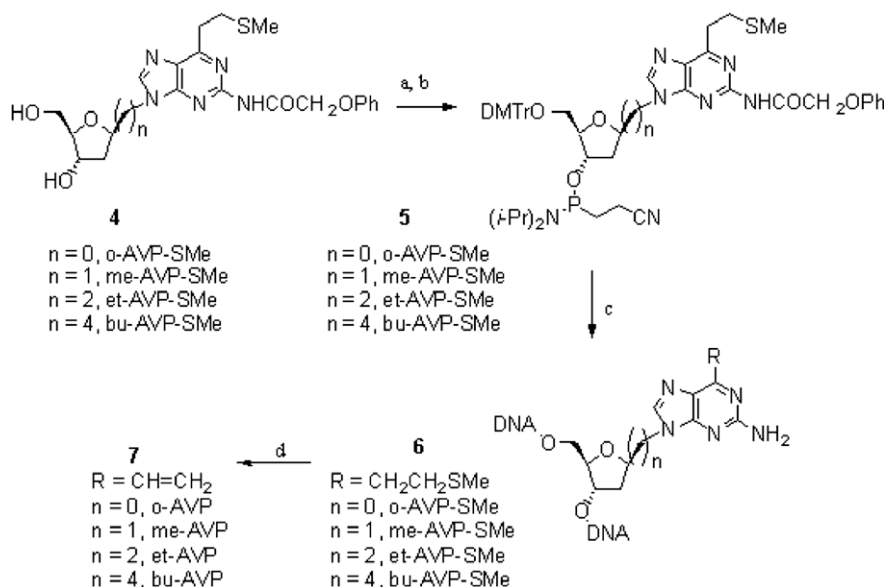
Scheme 3. Reagents and conditions: (a) DMTrCl, pyridine; (b) 2-cyanoethyl-*N*,*N*-diisopropylchlorophosphoramidite, DIPEA, CH_2Cl_2; (c) (1) synthesis with an automated DNA synthesizer; (2) 28% aqueous NH_3; (3) HPLC purification; (4) 10% CH_3COOH; (d) (1) 2 equiv MMPP; (2) aqueous NaOH.

Table 1
The sequences and MALDI-TOF MS results of oligonucleotides (**6**) containing reactive functional nucleoside derivatives in this study

ODN	Sequence	MALDI-TOF mass (*m/z*)	
		Calcd	Found
o-ODN(**8**)	5′ d(CTT T(**o-AVP-SMe**) T TCT CCT TTC T) 3′	4810.99	4809.95
me-ODN(**8**)	5′ d(CTT T(**me-AVP-SMe**) T TCT CCT TTC T) 3′	4825.02	4824.39
et-ODN(**8**)	5′ d(CTT T(**et-AVP-SMe**) T TCT CCT TTC T) 3′	4839.05	4837.73
bu-ODN(**8**)	5′ d(CTT T(**bu-AVP-SMe**) T TCT CCT TTC T) 3′	4867.11	4871.34
o-ODN(**9**)	5′ d(TAT ACT GAt CAA ATT (**o-AVP-SMe**) TA T)* 3′	6065.07	6071.17
et-ODN(**9**)	5′ d(TAT ACT GAt CAA ATT (**et-AVP-SMe**) TA T)* 3′	6093.10	6098.34
ODN(**10**)	5′ d(TTC GCC TCT TTG ATT AAC GCC) 3′	6319.98	6319.50
o-ODN(**10**)	5′ d(TTC GCC TCT TT (**o-AVP-SMe**)ATT AAC GCC) 3′	6378.00	6381.08
et-ODN(**10**)	5′ d(TTC GCC TCT TT (**et-AVP-SMe**)ATT AAC GCC) 3′	6406.03	6400.53
ODN(**11**)	5′ d(ATG CCC ATA CTG TTG AGC AAT)* 3′	6611.13	6610.10
o-ODN(**11**)	5′ d(ATG CCC ATA CT(**o-AVP-SMe**)TTG AGC AAT)* 3′	6669.15	6668.43
et-ODN(**11**)	5′ d((ATG CCC ATA CT(**et-AVP-SMe**)TTG AGC AAT)* 3′	6691.18	6696.54

* These oligonucleotides have an amino linker at the 3′ end.
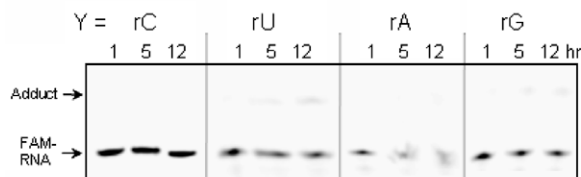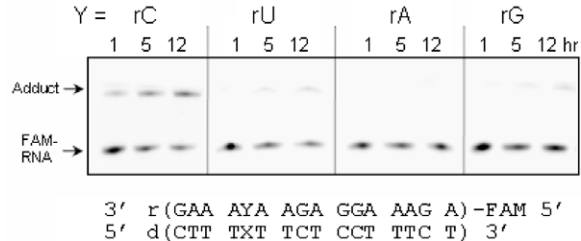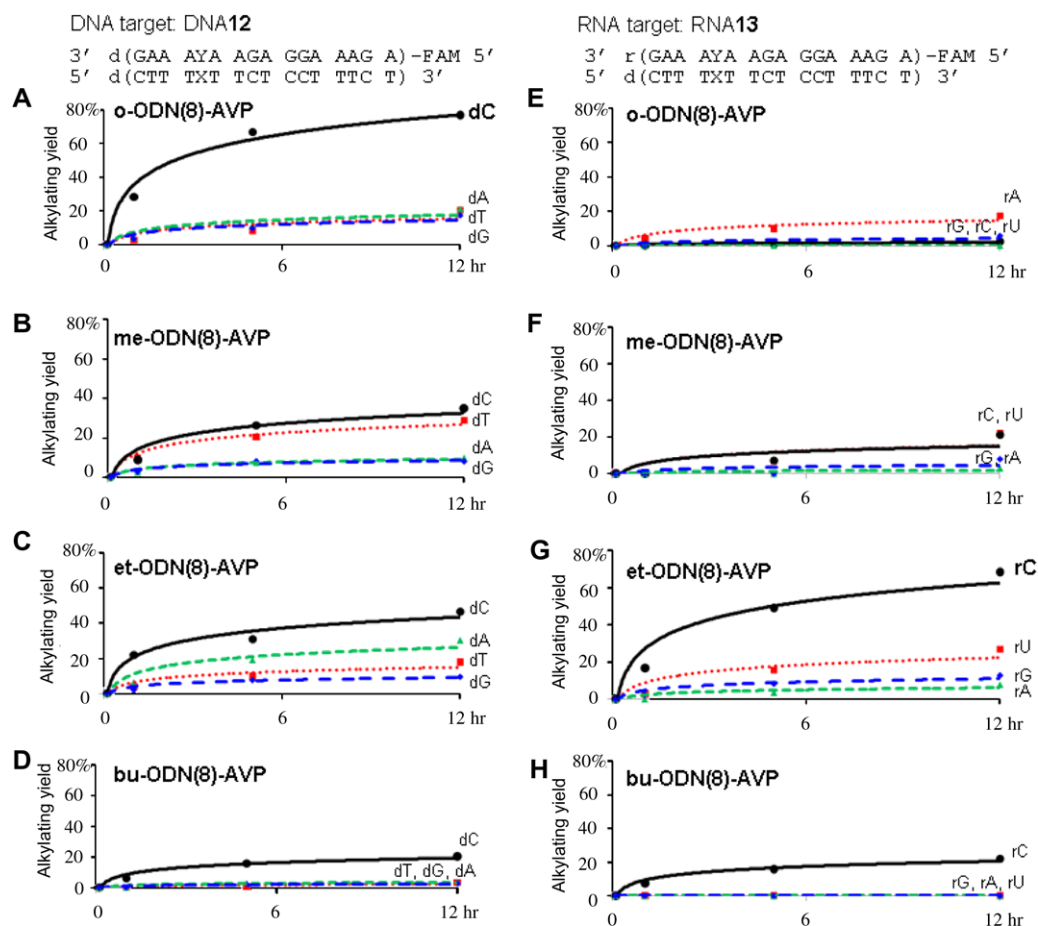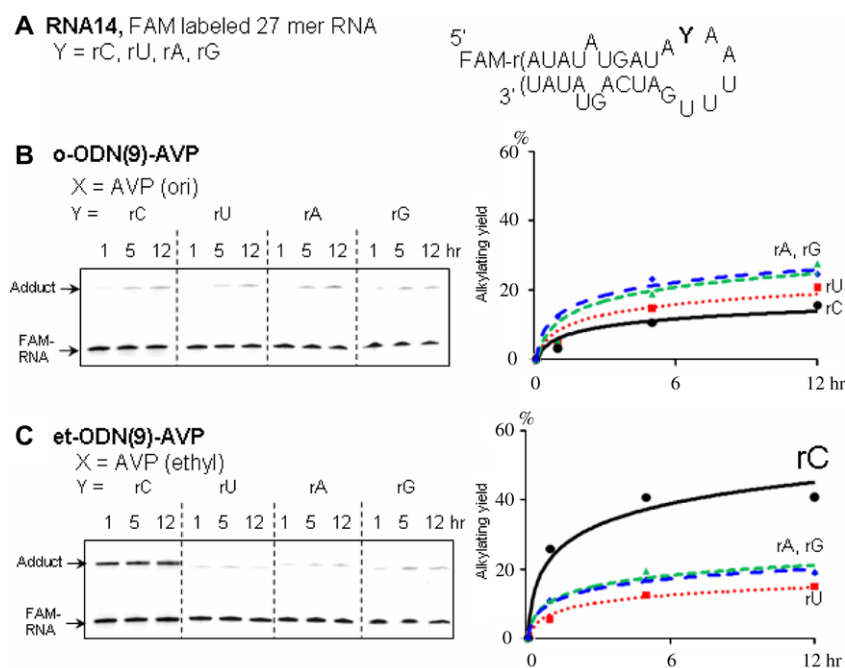

Figure 2. Gel shift assay to determine the crosslinking ability in the reaction buffer containing 100 mm NaCl, 50 mM MES pH 50. (A) o-ODN(**8**)-AVP and FAM-labeled 16 mer target RNA. (B) et-ODN(**8**)-AVP and FAM-labeled 16 mer target RNA.

displayed a selective crosslinking ability to rC, although the alkylating yield for the loop RNA is slightly lower than that with the linear RNA (Fig. 4C).

To further check the sequence dependency, the 27 mer FAM-labeled RNAs (FAM-RNA**15** and **16**) were designed as the model sequence of the luciferase mRNA. The time course of the crosslinking yields between FAM-RNA**15** with o-, et-ODN(**10**) is shown in Figure 5A, and those between FAM-RNA**16** and o-, et-ODN(**11**) are summarized in Figure 5B. Unexpected findings were that crosslinked products were formed in the reaction of FAM-RNA**15** having rU at the target site with o-ODN(**10**) and et-ODN(**10**), although the highest yields were obtained with et-ODN(**10**) toward rC at the target site of FAM-RNA**15** (Fig. 5A). The structure determination of the adduct with rU is needed for discussion of this unexpected crosslinking, but an alkylation with the carbonyl group of rU might be included like a new crosslinking agent for rU.[27] On the other hand, the results with the FAM-RNA**16** were consistent with the prediction of a low reactivity with o-ODN(**11**) and rC selectivity with et-ODN(**11**) (Fig. 5B). These results have clearly suggested that the sequence dependency of the original AVP analog has been overcome with the ethylene-linked AVP analog, but nevertheless, there is the still need to design a suitable RNA sequence for the target site of crosslinking.

DNA target: DNA**12**

3′ d(GAA AYA AGA GGA AAG A)-FAM 5′
5′ d(CTT TXT TCT CCT TTC T) 3′

RNA target: RNA**13**

3′ r(GAA AYA AGA GGA AAG A)-FAM 5′
5′ d(CTT TXT TCT CCT TTC T) 3′

Figure 3. Results of alkylating ability of 10 μM 16 mer oligonucleotides (o-ODN(**8**), me-ODN(**8**), et-ODN(**8**), bu-ODN(**8**)) having AVP derivatives for 1 μM FAM-labeled target DNA (A–D) and target RNA (E–H) (dC and rC black line, dT and rU red line, dA and rA green line, dG and rG blue line) in the reaction buffer containing 100 mM NaCl, 50 mM MES pH 5.0.


A RNA**14**, FAM labeled 27 mer RNA
Y = rC, rU, rA, rG

B o-ODN(**9**)-AVP
X = AVP (ori)

C et-ODN(**9**)-AVP
X = AVP (ethyl)

Figure 4. (A) The sequence and the second structure of the target RNA. (B) Gel results and crosslinking yield of the sequence o-ODN(**9**) containing o-AVP to the target RNA. (C) Gel results and crosslinking yield of the sequence et-ODN(**9**) containing et-AVP to the target RNA. o- and et-ODN(**9**): 5′ d(TATACTGATCAAATTXTAT). Conditions: 10 μM reactive ODNs, 1 μM FAM-labeled target RNA, 100 mM NaCl, 50 mM MES, pH 5 at 37 °C.
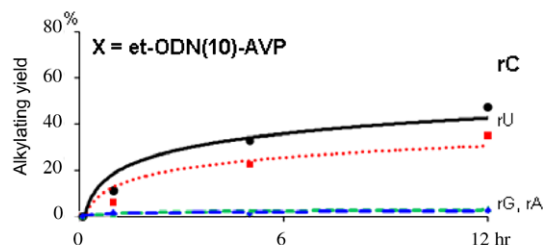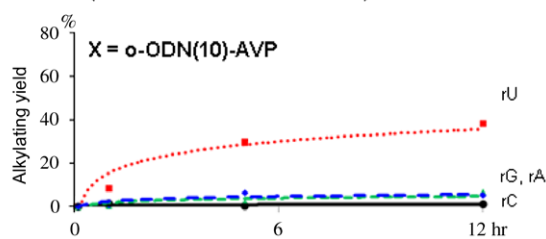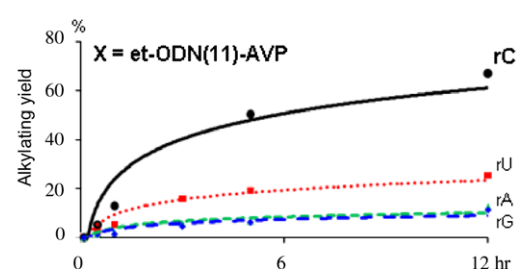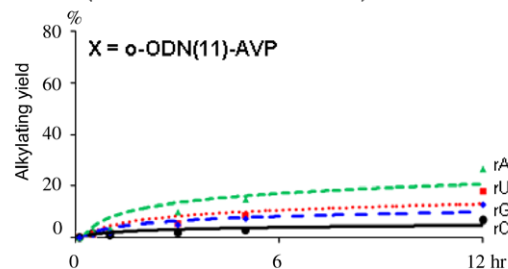
Figure 5. Crosslinking ability for the model sequence of luciferase mRNA. (A) The results of 21 mer 2′-deoxyoligonucleotides o-ODN(**10**) and et-ODN(**10**). (B) The results of 21 mer 2′-deoxyoligonucleotides o-ODN(**11**) and et-ODN(**11**). Conditions: 10 μM reactive ODNs, 1 μM FAM-labeled target RNA (Y = rC, rU, rA and rG), 100 mM NaCl, 50 mM MES, pH 5 at 37 °C.

2.3. The thermal stability and conformation of the DNA/RNA duplexes formed with the ODN containing the AVP analog

It may be assumed that the sequence dependency regarding the reactivity and the selectivity may arise from the thermal stability and the conformation of the duplexes. The thermal stability was estimated by measuring the melting temperature (T_m) of the duplex formed between the 21 mer ODN containing the AVP, ODN(**10** or **11**) with the 27 mer RNA, RNA**15**, or RNA**16** (Fig. 6A and B), and the results are summarized in Table 2. The T_m value of the RNA**15**/o-ODN(**10**) duplex was slightly lower than that of the RNA**15**/et-ODN(**10**) duplex, and both were lower than that of
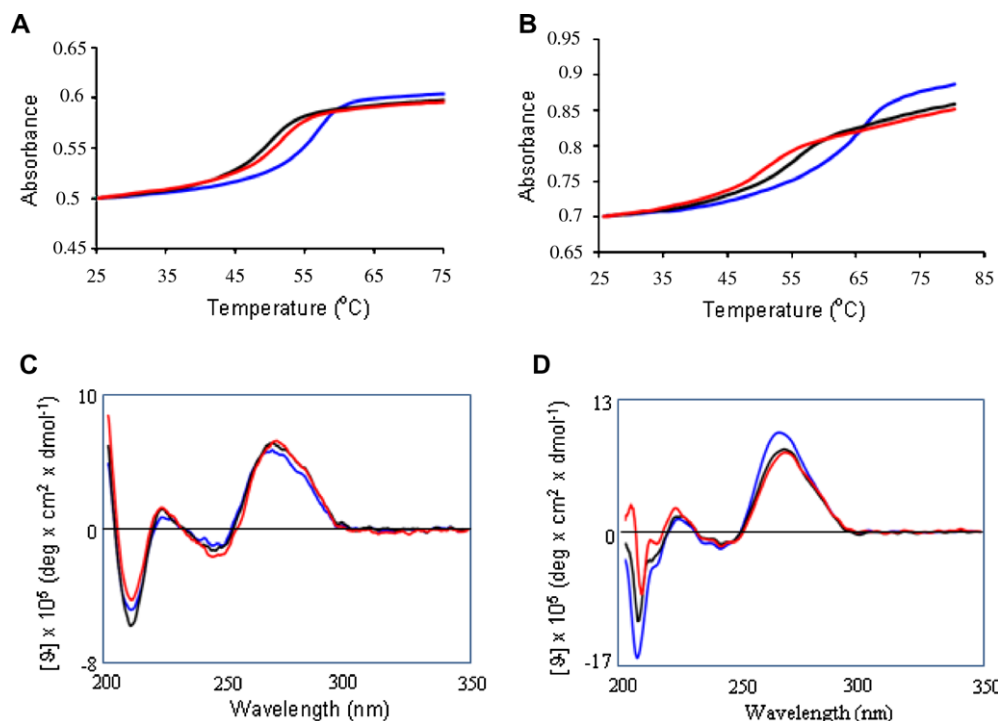
Figure 6. UV-melting curves (A and B) and CD spectra (C and D). A and C show ODN(**10**)/RNA**15** heteroduplex in blue line, o-ODN(**10**)/RNA**15** heteroduplex in black line and et-ODN(**10**)/RNA**15** heteroduplex in red line. B and D show ODN(**11**)/RNA**16** heteroduplex in blue line, o-ODN(**11**)/RNA**16** heteroduplex in black line and et-ODN(**11**)/RNA**16** heteroduplex in red line. The spectra were recorded in 100 mM NaCl, 50 mM MES buffer, pH 5.0 at room temperature. The concentration of each strand was 1.5 μM. The RNA sequences are described in Table 2.

Table 2
T_m values of functional nucleosides in ODN with complementary RNA[a]

DNA	Target RNA*	T_m (°C)
ODN(**10**)	RNA**15**	55.8
o-ODN(**10**)	RNA**15**	49.4
et-ODN(**10**)	RNA**15**	50.4
ODN(**11**)	RNA**16**	64.1
o-ODN(**11**)	RNA**16**	53.3
et-ODN(**11**)	RNA**16**	49.7

* RNA15: 5′ r(CGCUGGGCGUUAAUCAAAGAGGCGAAC) 3′.
* RNA16: 5′ r(ACGUGAAUUGUUCAACAGUAUGGGCAU) 3′.
[a] UV-melting profiles measured using 1.5 µM each of the strand in 100 mM NaCl, 50 mM MES buffer, pH 5.0.

the ODN(**10**)/RNA**15** duplex (55.8 °C). In the case of the duplex with RNA**16**, the T_m value with o-, et-ODN(**11**) was more than 10 °C lower than that with the natural ODN(**11**) containing dG instead of the AVP derivative. These results indicate that the duplex is destabilized by the alkylating structure regardless of the presence or absence of the alkyl linker. The RNA**16**/et-ODN(**11**) duplex produced a crosslinked product with a high rC selectivity, but gave only low T_m values. Accordingly, it was shown that the thermal stability of the duplex is not the major contributor of the crosslinking reactivity.

The circular dichroism spectra were measured to check the conformational change in the ODN/RNA heteroduplex. The CD spectra of the duplex formed with RNA**15** and ODN(**10**), o-ODN(**10**) and et-ODN(**10**) are compared in Figure 6C, and those formed with RNA**16** and ODN(**11**), o-ODN(**11**), and et-ODN(**11**) are shown in Figure 6D. All of these CD spectra indicate that the heteroduplexes are in between the A- and B-conformation and are similar to each other, suggesting that a large conformational change is not responsible for the difference in the crosslinking reactivity.

3. Discussion

This study aimed to develop an efficient crosslinking agent based on the 2-amino-6-vinylpurine (AVP) unit in order to crosslink with the RNA molecules. The AVP analogs were designed to connect the 2-amino-6-vinylpurine to the 2′-deoxyribose via a linker with a different length to optimize the linker length for better crosslinking efficiency.

Among the three linkers, the methylene, ethylene, and butylene linker, the best improvement in the crosslinking reactivity as well as the selectivity to rC was obtained with the ethylene linker analog, et-AVP. To the RNA targets where the original AVP did not produce a significant crosslinked product, et-AVP produced the crosslinked products in high yield with a high rC selectivity. The sequence dependency of the reactivity of the original AVP to rC in RNA has been overcome by et-AVP, although some limitations still remain. The high reactivity of et-AVP toward rC in RNA compared to the original AVP cannot be explained either by the difference in the thermal stability or the difference in the duplex conformation. Generally, the geometries of the GC and AT base pairs are almost same in the DNA/DNA duplex and the DNA/RNA heteroduplex. However, it is apparent that a slight difference in the geometry of AVP to the rC complex significantly affected the alkylating ability of the AVP analogs. The thermal denaturing study and the CD results have shown that the DNA/RNA heteroduplex is between the A- and B-type conformation with only a slight distortion because of o-AVP-SMe and et-AVP-SMe. It has been proposed by MD calculation that base pairs in duplex RNA experience local opening events into the major groove, while such events are not simulated in the DNA duplex.[28] In the DNA/RNA heteroduplex in the conformation between A- and B-type, the 2-amino-6-vinylpurine base may cause such a conformational change to open the AVP-cytosine mismatch base pair and push the cytosine base into the major groove (Fig. 7, A1 vs. A2). In such a conformation, the amino group of the cytosine base is no longer in close proximity with the vinyl group of the original AVP without the linker. On the other hand, the ethylene-linked 2-amino-6-vinylpurine base (et-AVP) might reach the cytosine base in a distorted conformation (Fig. 7, B1 vs. B2). Although there is no experimental evidence, it may be speculated that the ethylene linker makes the 2-amino-6-vinyl purine unit flexible in order to adjust the movement of the cytosine base. In conclusion, it has been clearly shown that the nucleoside analog, et-AVP, having the 2-amino-6-vinylpurine unit through the ethylene linker is an efficient and selective crosslinking agent to the rC in the RNA target.
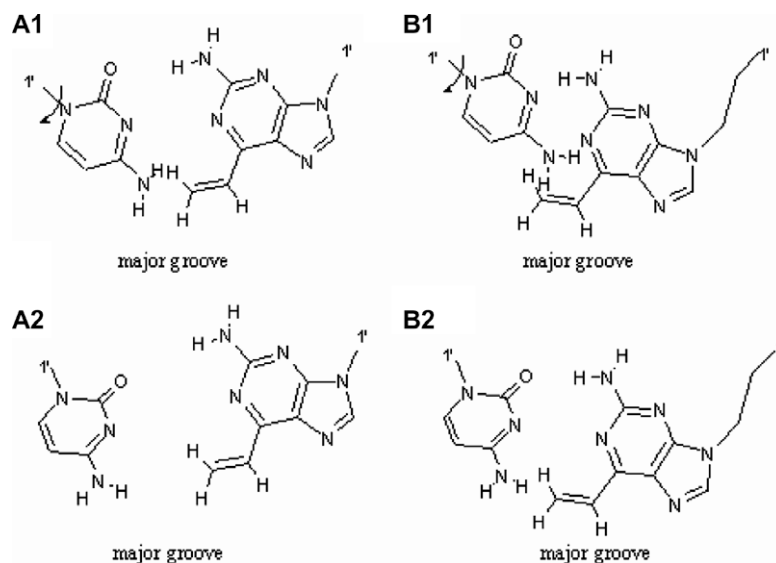
Figure 7. Schematic representations of the 2-amino-6-vinylpurine and the cytosine base (A1 and A2) and the ethylene-linked 2-amino-6-vinylpurine and the cytosine base (B1 and B2). In A1 and B1, the cytosine base is located at a natural conformation in DNA/RNA duplex (A1 and A2). A2 and B2 illustrate the cytosine base slightly flipped out to the major groove. Only bases are shown for clarity.

4. Materials and methods

4.1. General

All reactions were performed under an argon atmosphere. The
^{1}H NMR (400 and 500 MHz) spectra were recorded by a Varian
UNITY-400 and INOVA-500 spectrometer, respectively. The ^{31}P
NMR (161 MHz) spectrum was recorded using 10% phosphoric acid
in D_2O for the internal standard at 0 ppm. The IR spectra were ob-
tained using a Perkin Elmer FTIR-SpectrumOne. The high-resolu-
tion mass spectra were recorded by an Applied Biosystems
Mariner System 5299 spectrometer. The MALDI-TOF mass spectra
were recorded by a Bruker Daltonics Microflex instrument.

4.1.1. 2-Deoxy-1-tosyloxymethyl-3,5-O-ditoluoyl-β-D-ribofuranose (2)

A solution of **1** (814 mg, 2.15 mmol), 1,4-dioxane (20 ml), and a
36% aqueous HCl solution (1.87 ml) was refluxed at 80 °C for 2 h.
The reaction mixture was quenched with a satd $NaHCO_3$ solution
and extracted with $CHCl_3$. The organic layer was dried over Na_2SO_4,
and evaporated. The residue was dissolved in THF and cooled to
0 °C. The BH_3–THF complex (9.7 ml, 9.65 mmol) was slowly added
to this solution at 0 °C. After stirring for 1.5 h at room temperature,
the reaction mixture was quenched with a 10% aqueous HCl solu-
tion and extracted with $CHCl_3$. The organic layer was dried over
Na_2SO_4, and then evaporated. The residue was purified by silica-
gel column chromatography (hexane/EtOAc = 1:1) to give a color-
less oil (680 mg, 1.72 mmol, 80% for two steps). p-Toluenesulfonyl
chloride (p-TsCl) (476 mg, 2.5 mmol) was added to a solution of the
colorless oil (600 mg, 1.56 mmol) in pyridine (6.0 ml) at 0 °C. After
stirring for 24 h, the reaction mixture was poured into ice water
and extracted with $CHCl_3$. The organic layer was dried over Na_2SO_4,
and evaporated. The residue was purified by silica-gel column
chromatography (hexane/EtOAc = 1:1) to give **2** as a pale yellow
oil (693 mg, 1.29 mmol, 83%). ^{1}H NMR (400 MHz, CDCl$_3$): δ 7.92–
7.87 (4H, m), 7.77–7.75 (2H, m), 7.28–7.22 (6H, m), 5.44 (1H, d,
J = 4.0 Hz), 4.48–4.30 (2H, m), 4.21–4.09 (2H, m), 2.41 (3H, s),
2.40 (3H, s), 2.35 (3H, s), 2.24–2.12 (2H, m). FTIR (neat): 1718,
1270 cm^{-1}. ESI-MS: 539.08 (M+H)$^+$.

4.1.2. 2-Amino-9-[2-(2′-deoxy-β-D-ribofuranosyl)methyl]-6-(2-methylthioethyl)purine (3)

2-Amino-6-chloropurine (432 mg, 2.55 mmol) was added to a
solution of potassium t-butoxide (301 mg, 2.55 mmol) in dimethyl-
sulfoxide (DMSO) (5.0 ml). After stirring for 1.5 h, a solution of **2**
(686 mg, 1.27 mmol) in DMSO (5.0 ml) was added to the above mix-
ture, then the reaction mixture was refluxed for 3 h at 80 °C. The
reaction mixture was quenched with satd ammonium chloride solu-
tion and extracted with EtOAc. The organic layer was successively
washed with water and brine, dried over Na_2SO_4, and evaporated.
The residue was purified by silica-gel column chromatography (hex-
ane/EtOAc = 1:1) to give a colorless oil (357 mg, 0.67 mmol, 52%).
Tetrakis(triphenylphosphine)palladium(0) (70.5 mg, 0.061 mmol),
lithium bromide (64.9 mg, 0.73 mmol), potassium bicarbonate
(50.8 mg, 0.37 mmol), and 2,4,6-trivinylcyclotriboroxane pyridine
complex (212 mg, 0.85 mmol) were added to a solution of the color-
less oil (327 mg, 0.61 mmol) in water/dioxane = 1:3 (11.5 ml). The
reaction mixture was refluxed for 1 h at 120 °C, and quenched with
a satd ammonium chloride solution and extracted with EtOAc. The
organic layer was successively washed with water and brine, dried
over Na_2SO_4, and evaporated to give a brown caramel (506 mg). This
brown caramel solution in acetonitrile (5.0 ml) was treated with
sodium methanethiolate solution (0.43 ml, 0.92 mmol) for 15 min.
The reaction mixture was diluted with $CHCl_3$. The organic layer
was continuously washed with water and brine, dried over Na_2SO_4,

and evaporated. The residue was purified by silica-gel column
chromatography (hexane/EtOAc = 1:2 to 1:1 to EtOAc only) to give
3 as a yellow caramel (330 mg, 0.57 mmol, 94%). ^{1}H NMR
(400 MHz, CDCl$_3$): δ 7.90–7.83 (4H, m), 7.85 (1H, s), 7.25–7.20
(4H, m), 5.46 (1H, d, J = 6.1 Hz), 5.18 (2H, bs), 4.56–4.52 (2H, m),
4.45–4.36 (2H, m), 3.33–3.19 (1H, m), 3.02–3.00 (1H, m), 2.41 (3H,
s), 2.40 (3H, s), 2.38–2.29 (1H, m), 2.17 (3H, s), 2.13–1.96 (1H, m).
FTIR (neat): 1716, 1610 cm^{-1}. ESI-MS: 570.20 (M+H)$^+$.

4.1.3. 9-[2-(2′-Deoxy-β-D-ribofuranosyl)methyl]-6-(2-methylthioethyl)-2-phenoxyacetyl-aminopurine (4)

Sodium methoxide (153 mg, 2.7 mmol) was added to a solution
of **3** (155 mg, 0.27 mmol) in MeOH (7.0 ml), then the reaction mix-
ture was refluxed at 70 °C for 1 h. The reaction mixture was
quenched with a satd ammonium chloride solution and extracted
with EtOAc. The organic layer was continuously washed with
water and brine, dried over Na_2SO_4, and evaporated. The residue
was dissolved in pyridine/CH_2Cl_2 = 1:3 (6.4 ml) and cooled to 0 °C
in an ice bath. Trimethylsilyl chloride (0.34 ml, 2.69 mmol) was
added to this mixture. After stirring for 1.5 h at room temperature,
the mixture was cooled to 0 °C again. Phenoxyacetyl chloride
(37 μl, 0.39 mmol) was added to this mixture at 0 °C. The reaction
mixture was stirred for 3 h at the same temperature, and diluted
with CH_3OH (1.6 ml). After stirring for 12 h at room temperature,
the reaction mixture was diluted with $CHCl_3$. The organic layer
was washed with water, dried over Na_2SO_4, and evaporated. The
residue was purified by silica-gel column chromatography
(CHCl$_3$/CH$_3$OH = 10:1) to give **4** as a colorless caramel (86.4 mg,
0.18 mmol, 68% for two steps). ^{1}H NMR (400 MHz, CDCl$_3$): δ 9.10
(1H, s), 8.09 (1H, s), 7.34–7.30 (2H, m), 7.05–7.00 (3H, m), 6.83
(1H, d, J = 6.3 Hz), 4.78–4.74 (2H, m), 4.54–4.50 (1H, m), 4.44–
4.39 (2H, m), 4.30–4.27 (1H, m), 3.85 (1H, d, J = 3.4 Hz), 3.64–
3.55 (2H, m), 3.43–3.39 (2H, m), 3.07–3.03 (2H, m), 2.16 (3H, s),
2.13–2.09 (1H, m), 1.96–1.92 (1H, m). FTIR (neat): 3379, 2918,
1691, 1600 cm^{-1}. ESI-MS: 474.24 (M+H)$^+$.

4.1.4. 9-[2-(2′-Deoxy-3′-O-N,N-diisopropylcyanoethylphosphor-amidyl-5′-O-(4,4′-dimethoxytrityl)β-D-ribofuranosyl)methyl]-6-(2-methylthioethyl)-2-phenoxyacetylaminopurine (5)

DMTrCl (92 mg, 0.26 mmol) was added to a solution of **4**
(96 mg, 0.2 mmol) in pyridine containing molecular sieves 4 Å.
After stirring for 1 h, the reaction mixture was diluted with
$CHCl_3$, and then washed with water and brine. The organic layer
was washed with water and brine, dried over Na_2SO_4, evapo-
rated, and then the residue was purified by silica-gel column
chromatography (CHCl$_3$ containing 0.5% pyridine) to give the
DMTr-protected compound (96.1 mg, 0.12 mmol, 61%). Subse-
quently, iP$_2$NEt (67 μl, 0.39 mmol) was added to this solution
of the DMTr-compound (50 mg, 0.06 mmol) and iPr$_2$NP(-
Cl)OC$_2$H$_4$CN (43 μl, 0.19 mmol) in CH_2Cl_2 at 0 °C. After stirring
for 30 min, the reaction mixture was diluted with a satd NaH-
CO$_3$ solution, and extracted with EtOAc. The organic layer was
dried over Na_2SO_4, evaporated, and then the residue was puri-
fied by flash silica-gel column chromatography (hexane/
EtOAc = 2:1) to give **5** as a white powder (39 mg, 0.04 mmol,
62%). ^{1}H NMR (400 MHz, CDCl$_3$): δ 8.88 (1H, bs), 8.12 (1H, s),
7.43–7.28 (10H, m), 7.23–7.19 (2H, m), 7.06–7.01 (3H, m),
6.83 (4H, dd, J = 7.0, 1.5 Hz), 4.80–4.78 (2H, m), 4.59–4.39 (3H,
m), 4.19–4.11 (3H, m), 3.79 (3H, s), 3.78 (3H, s), 3.74–3.68
(1H, m), 3.66–3.57 (1H, m), 3.54–3.48 (2H, m), 3.46–3.39 (2H,
m), 3.16–3.15 (2H, m), 3.07 (2H, t, J = 7.63 Hz), 2.75 (1H, t,
J = 6.41 Hz), 2.40 (1H, t, J = 6.41 Hz), 2.18 (3H, s), 1.14 (6H, d,
J = 6.72 Hz), 1.10 (6H, d, J = 6.72 Hz). FTIR (neat): 2967, 2364,
1697, 1600 cm^{-1}. ESI-MS: 976.71 (M+H)$^+$. ^{31}P NMR (161 MHz,
CDCl$_3$): δ 148.7, 148.5.

4.2. Oligonucleotides (6)

The 2′-deoxy oligonucleotides (ODNs) containing the AVP derivative were synthesized using an automated DNA synthesizer (Applied Biosystems 394 DNA/RNA synthesizer) on a 1.0 μmol scale. The synthesized ODNs were cleaved from CPG by 28% aqueous ammonium hydroxide at room temperature and purified by HPLC (conditions: column, Nacalai Tesque COSMOSIL 5C18AR-II 10×250 mm; flow rate, 3.0 ml/min; buffer A, 0.1 M TEAA; B, CH_3CN; B concentration 10–40%/20 min, 40–100%/30 min, linear gradient). The DMTr-protecting groups of the purified ODNs were removed by 10% acetic acid and the formed DMTrOH was extracted with Et_2O. The structure of the synthetic ODNs was confirmed by a MALDI-TOF MS measurement. The MALDI-TOF MS results are summarized in Table 1.

4.3. The crosslinking reaction and the analysis by denatured polyacrylamide gel

The methylthio group of ODN in the oligonucleotides **6** was converted to the vinyl group **7** by MMPP (2.0 equiv) and aqueous sodium hydroxide at room temperature. The RNase OUT (40 unit), reaction buffer (final concd; 100 mM NaCl and 50 mM MES, pH 5) and FAM-labeled target DNA or RNA (50 pmol) were added to the above mixture at 0 °C. The reaction mixture was incubated at 37 °C, and the reaction was stopped by mixing with a buffer (95% formamide, 20% EDTA, 0.05% bromophenol blue) at the appropriate time. The reaction progress was analyzed by electrophoresis with 15% denatured polyacrylamide gel containing 7 M urea, and the intensity of FAM-labeled bands were quantified by a luminescent image analyzer LAS-3000 (Fujifilm).

4.4. Thermal denaturing study (T_m value)

A mixture of the corresponding ODN **6** (1.5 μM) and 27 mer of the complimentary RNA (1.5 μM) in the buffer (100 mM NaCl and 50 mM MES, pH 5) was heated at 85 °C for 10 min then slowly cooled. The melting curve was obtained by warming a sample at the rate of 1.0 °C/min from 20 to 80 °C with monitoring at 260 nm by a UV–vis spectrophotometer, DU 800 (Beckman Coulter). The data were analyzed by the melt curve processing program, MeltWin v. 3.5.

4.5. Circular dichroism (CD) spectroscopy

The CD spectra were measured by a JASCO J-720W spectrophotometer at room temperature in a cylindrical quartz cell with a path length of 0.1 cm. The samples were prepared in the same manner as described in the thermal denaturing study. The Spectra were converted to a molar ellipticity, which was performed by the JASCO standard analysis software.

References and notes

1. Matsubara, H.; Takeuchi, T.; Nishikawa, E.; Yanagisawa, K.; Hayashita, Y.; Ebi, H.; Yamada, H.; Suzuki, M.; Nagino, M.; Nimura, Y.; Osada, H.; Takahashi, T. *Oncogene* **2006**, *26*, 6099.
2. Stenvang, J.; Lindow, M.; Kauppinen, K. *Biochem. Soc. Trans.* **2008**, *36*, 1197.
3. Horwich, M. D.; Zamore, P. D. *Nat. Protoc.* **2008**, *3*, 1537.
4. Fei, J. L.; Feiei, G.; Ming, L. Y.; Liu, Y. *J. Drug Target* **2008**, *16*, 688.
5. Yu, R. Z.; Lemonidis, K. M.; Graham, M. J.; Matson, J. E.; Crooke, R. M.; Tribble, D. L.; Wedel, M. K.; Levin, A. A.; Geary, R. S. *Biochem. Pharmacol.* **2009**, *77*, 910–919.
6. Crooke, S. T. In *Antisense Drug Technology Principles, Strategies, and Applications*, 2nd ed.; CRC Press: Boca Raton, 2007.
7. Aboul-Fadl, T. *Expert Opin. Drug Discov.* **2006**, *1*, 285.
8. Elmén1, J.; Lindow, M.; Schütz, S.; Lawrence, M.; Petri, A.; Obad, S.; Lindholm, M.; Hedtjärn, M.; Hansen, H. F.; Berger, U.; Gullans, S.; Kearney, P.; Sarnow, P.; Straarup, E. M.; Kauppinen, S. *Nature* **2008**, *452*, 896.
9. Elmén, J.; Lindow, M.; Silahtaroglu, A.; Bak, M.; Christensen, M.; Lind-Thomsen, A.; Hedtjärn, M.; Hansen, J. B.; Hansen, H. F.; Straarup, E. M.; McCullagh, K.; Kearney, P.; Kauppinen, S. *Nucleic Acids Res.* **2008**, *36*, 1153.
10. Tillman, L. G.; Geary, R. S.; Hardee, G. E. *J. Pharm. Sci.* **2008**, *97*, 225.
11. Davis, S.; Propp, S.; Freier, S. M.; Jones, L. E.; Serra, M. J.; Kinberger, G.; Bhat, B.; Swayze, E. E.; Bennett, C. F.; Esau, C. *Nucleic Acids Res.* **2009**, *37*, 70.
12. Nagatsugi, F.; Uemura, K.; Nakashima, S.; Maeda, M.; Sasaki, S. *Tetrahedron Lett.* **1995**, *36*, 421.
13. Nagatsugi, F.; Uemura, K.; Nakashima, S.; Maeda, M.; Sasaki, S. *Tetrahedron* **1997**, *53*, 3035.
14. Nagatsugi, F.; Kawasaki, T.; Usui, D.; Maeda, M.; Sasaki, S. *J. Am. Chem. Soc.* **1999**, *121*, 6753.
15. Kawasaki, T.; Nagatsugi, F.; Ali, M. M.; Maeda, M.; Sugiyama, K.; Hori, K.; Sasaki, S. *J. Org. Chem.* **2005**, *70*, 14.
16. Ali, M. M.; Oishi, M.; Nagatsugi, F.; Mori, K.; Nagasaki, Y.; Kataoka, K.; Sasaki, S. *Angew. Chem., Int. Ed.* **2006**, *45*, 3136.
17. Ali, M. M.; Nagatsugi, F.; Sasaki, S.; Nakahara, R.; Maeda, M. *Nucleosides, Nucleotides, Nucleic Acids* **2006**, *25*, 159.
18. Nagatsugi, F.; Nakahara, R.; Inoue, K.; Sasaki, S. *Arch. Pharm. Chem. Life Sci.* **2008**, *341*, 562.
19. Ali, M. M.; Imoto, S.; Li, Y.; Sasaki, S.; Nagatsugi, F. *Bioorg. Med. Chem.* **2009**, *17*, 2859.
20. Nagatsugi, F.; Sasaki, S.; Miller, P. S.; Seidman, M. M. *Nucleic Acids Res.* **2003**, *31*, e31.
21. Nagatsugi, F.; Matsuyama, Y.; Maeda, M.; Sasaki, S. *Bioorg. Med. Chem. Lett.* **2002**, *12*, 487.
22. Nagatsugi, F.; Usui, D.; Kawasaki, T.; Maeda, M.; Sasaki, S. *Bioorg. Med. Chem. Lett.* **2001**, *11*, 343.
23. Grünefeld, P.; Richert, C. *J. Org. Chem.* **2004**, *69*, 7543.
24. Adamo, M. F. A.; Adlington, R. M.; Baldwin, J. E.; Day, A. L. *Tetrahedron* **2004**, *60*, 841.
25. Nagatsugi, F.; Ogata, Y.; Imoto, S.; Sasaki, S. *Heterocycles* **2007**, *73*, 493.
26. Fan, F.; Gaffney, B. L.; Jones, R. A. *Org. Lett.* **2004**, *6*, 2555.
27. Hattori, K.; Hirohama, T.; Imoto, S.; Kusano, S.; Nagatsugi, F. *Chem. Commun.* **2009**, 6463.
28. Pan, Y.; MacKerell, A. D., Jr. *Nucleic Acids Res.* **2003**, *31*, 7131.